PHYSICAL REVIEW D **88,** 055026 (2013)

Electroweak versus high-scale fine tuning in the 19-parameter supergravity model

Howard Baer,[1,*] Vernon Barger,[2,†] and Maren Padeffke-Kirkland[1,‡]

[1]*Department of Physics and Astronomy, University of Oklahoma, Norman, Oklahoma 73019, USA*

[2]*Department of Physics, University of Wisconsin, Madison, Wisconsin 53706, USA*

(Received 18 June 2013; published 30 September 2013)

Recently, two measures of electroweak fine tuning (EWFT) have been introduced for (supersymmetry) SUSY models: $\Delta_{\rm EW}$ compares the Z mass to each separate weak scale contribution to m_Z, while $\Delta_{\rm HS}$ compares the Z mass to high scale input parameters and their consequent renormalization group evolution ($1/\Delta$ is the percent of fine tuning). While the paradigm mSUGRA/CMSSM model has been shown to be highly fine tuned under both parameters ($\Delta_{\rm EW} \gtrsim 10^2$ and $\Delta_{\rm HS} \gtrsim 10^3$), the two-parameter nonuniversal Higgs model (NUHM2) in the context of radiatively driven natural SUSY (RNS) enjoys $\Delta_{\rm EW}$ as low as 10, while $\Delta_{\rm HS}$ remains $\gtrsim 10^3$. We investigate fine tuning in the 19-free-parameter SUGRA model (SUGRA19). We find that with 19 free parameters, the lowest $\Delta_{\rm EW}$ points are comparable to what can be achieved in NUHM2 with just six free parameters. However, in SUGRA19, $\Delta_{\rm HS}$ can now also reach as low as 5–10. The conditions which lead to low $\Delta_{\rm HS}$ include $m_{H_u} \sim m_Z$ at the high scale, with nonuniversal gaugino masses $M_{1,2} \gg M_3$ also at $m_{\rm GUT}$. The low $\Delta_{\rm HS}$ models are severely constrained by the $b \to s\gamma$ branching fraction. In both cases of low $\Delta_{\rm EW}$ and $\Delta_{\rm HS}$, the superpotential μ parameter should be $\sim$100–300 GeV. While SUSY models with low EWFT may or may not be discoverable at the LHC, the predicted light Higgsinos must show up at a linear e^+e^- collider with $\sqrt{s} \gtrsim 2|\mu|$.

DOI: 10.1103/PhysRevD.88.055026 PACS numbers: 14.80.Ly, 12.60.Jv, 11.30.Pb

I. INTRODUCTION

Supersymmetric models of particle physics are renown for providing an elegant solution to the daunting gauge hierarchy problem. They also receive indirect experimental support from (1) the measured strengths of weak scale gauge couplings, which allow for unification at a scale $m_{\rm GUT} \simeq 2 \times 10^{16}$ GeV within the Minimal Supersymmetric Standard Model (MSSM), and (2) the measured value of the top-quark mass, which is sufficiently high so as to radiatively drive electroweak symmetry breaking (REWSB) [1]. Along with these plaudits, (3) the recent discovery by Atlas [2] and CMS [3] of a Higgs-like boson with mass $m_h \simeq 125$ GeV confirms predictions from models of weak scale supersymmetry [4] where (in the context of the MSSM) a value $m_h \sim$ 114–135 GeV was required [5]. The emergent picture is that the MSSM (or possible extensions) may provide a solid description of nature not only at the weak scale, but perhaps all the way up to energy scales associated with grand unification [6].

Such an audacious extrapolation has suffered a string of serious setbacks: so far, no signs of supersymmetric matter have emerged from LEP, LEP2, Tevatron or, more recently, LHC data. Recent analyses from Atlas and CMS in the context of the minimal supergravity (mSUGRA or CMSSM) model [7] require $m_{\tilde{g}} \gtrsim 1.4$ TeV for $m_{\tilde{q}} \sim m_{\tilde{g}}$ and $m_{\tilde{g}} \gtrsim 1$ TeV for $m_{\tilde{g}} \ll m_{\tilde{q}}$. Naively, these results exacerbate the so-called little hierarchy problem (LHP) [8]: why is there an apparent discrepancy between the weak scale (typified by $m_Z \simeq 91.2$ GeV) and the SUSY scale, where m(sparticle) $\gtrsim 1$ TeV? The growing scale mismatch has led some physicists to call into question whether or not weak scale SUSY really exists, or at least to concede that it suffers unattractive electroweak fine tunings (EWFT) [9].

Traditionally, EWFT has been quantified using the Barbieri-Giudice measure [10–24]

$$\Delta_{\rm BG} \equiv \max_i \left| \frac{\partial \ln m_Z^2}{\partial \ln a_i} \right| \tag{1}$$

where a_i represents various fundamental parameters of the theory, usually taken to be some set of soft SUSY breaking parameters defined at some high energy scale $\Lambda_{\rm HS}$ below which the theory in question is posited to be the correct effective field theory description of nature. The quantity $1/\Delta$ is the percent of fine tuning. The value of $\Delta_{\rm BG}$ then answers the following question: how stable is the fractional Z-boson mass against fractional variation of high-scale model parameters? Depending on which parameters are included in the set a_i, very different answers emerge [24]. In addition, theories which are defined at very different values of $\Lambda_{\rm HS}$, but which nonetheless lead to exactly the same weak scale sparticle mass spectra, give rise to very different values of $\Delta_{\rm BG}$.

A. $\Delta_{\rm EW}$ and $\Delta_{\rm HS}$

Recently, two different measures of EWFT—$\Delta_{\rm EW}$ and $\Delta_{\rm HS}$—have been proposed which answer a different but related question: how is it possible that m_Z has a value of just 91.2 GeV while gluino and squark masses exist at TeV

*baer@nhn.ou.edu
†barger@pheno.wisc.edu
‡m.padeffke@ou.edu

or even far beyond TeV values? The answer should be as follows: those independent contributions which enter the scalar potential and conspire to build up the Z-boson mass should all be comparable to m_Z.

Minimization of the scalar potential in the MSSM [4] leads to the well-known relation that

$$\frac{m_Z^2}{2} = \frac{m_{H_d}^2 + \Sigma_d^d - (m_{H_u}^2 + \Sigma_u^u)\tan^2\beta}{\tan^2\beta - 1} - \mu^2, \quad (2)$$

where $m_{H_u}^2$ and $m_{H_d}^2$ are soft SUSY breaking (not physical) Higgs mass terms, μ is the superpotential Higgsino mass term, $\tan\beta \equiv v_u/v_d$ is the ratio of Higgs field vevs, and Σ_u^u and Σ_d^d include a variety of independent radiative corrections [25].

1. $\Delta_{\rm EW}$

Noting that all entries in Eq. (2) are defined at the weak scale, the electroweak fine-tuning parameter

$$\Delta_{\rm EW} \equiv \max_i |C_i|/(m_Z^2/2) \quad (3)$$

may be constructed, where $C_{H_d} = m_{H_d}^2/(\tan^2\beta - 1)$, $C_{H_u} = -m_{H_u}^2\tan^2\beta/(\tan^2\beta - 1)$ and $C_\mu = -\mu^2$. Also, $C_{\Sigma_u^u(k)} = \Sigma_u^u(k)/(m_Z^2/2)$ and $C_{\Sigma_d^d(k)} = \Sigma_d^d(k)/(m_Z^2/2)$, where k labels the various loop contributions included in Eq. (2). A low value of $\Delta_{\rm EW}$ means less fine tuning; e.g. $\Delta_{\rm EW} = 20$ corresponds to $\Delta_{\rm EW}^{-1} = 5\%$ fine tuning amongst terms contributing to $m_Z^2/2$. Since C_{H_d} and $C_{\Sigma_d^d(k)}$ terms are suppressed by $\tan^2\beta - 1$, for even moderate $\tan\beta$ values the expression Eq. (2) reduces approximately to

$$\frac{m_Z^2}{2} \simeq -(m_{H_u}^2 + \Sigma_u^u) - \mu^2. \quad (4)$$

In order to achieve low $\Delta_{\rm EW}$, it is necessary that $-m_{H_u}^2$, $-\mu^2$ and each contribution to $-\Sigma_u^u$ all be close to $m_Z^2/2$ to within a factor of a few.

A scan over mSUGRA/CMSSM parameter space, requiring that LHC sparticle mass constraints and $m_h = 125 \pm 2$ GeV be obeyed, finds a minimal value of $\Delta_{\rm EW} \sim 10^2$, with more common values being $\Delta_{\rm EW} \sim 10^3$–$10^4$. Thus, one may conclude that the Z mass is rather highly fine tuned in this paradigm model. In the case of mSUGRA, the value C_μ becomes low only in the hyperbolic branch/focus point [16,18] (HB/FP) region. In this region, however, m_0 and consequently $m_{\tilde{t}_{1,2}}$ are very large, so that $\Sigma_u^u(\tilde{t}_{1,2})$ are each large, and the model remains fine tuned.

Alternatively, if one moves to the two-parameter nonuniversal Higgs model (NUHM2) [26], with free parameters

$$m_0, \quad m_{1/2}, \quad A_0, \quad \tan\beta, \quad \mu, \quad m_A \quad (5)$$

then

(1) μ can be chosen in the 100–300 GeV range since it is now a free input parameter,

(2) a value of $m_{H_u}^2(m_{\rm GUT}) \sim (1.3$–$2.5)m_0$ may be chosen so that $m_{H_u}^2$ is driven only slightly negative at the weak scale, leading to $m_{H_u}^2({\rm weak}) \sim -m_Z^2/2$, and

(3) with large stop mixing from $A_0 \sim \pm 1.6m_0$, the top-squark radiative corrections are softened while m_h is raised to the $\sim$125 GeV level [25].

In the NUHM2 model, $\Delta_{\rm EW}$ as low as 5–10 can be generated. For such cases, the little hierarchy problem seems to disappear. The low $\Delta_{\rm EW}$ models are typified by the presence of light Higgsinos $m_{\tilde{W}_1}^{\pm}$, $m_{\tilde{Z}_{1,2}} \sim$ 100–300 GeV, which should be accessible to a linear e^+e^- collider operating with $\sqrt{s} \gtrsim 2|\mu|$. Also, $m_{\tilde{g}} \sim$ 1–5 TeV while $m_{\tilde{t}_1} \sim$ 1–2 TeV and $m_{\tilde{t}_2} \sim$ 2–4 TeV.

The measure $\Delta_{\rm EW}$ listed above is created from weak scale MSSM parameters and so contains no information about any possible high-scale origin, even though low values of $\Delta_{\rm EW}$ may be required of high-scale models: in this sense, low $\Delta_{\rm EW}$ captures a *minimal* EWFT required of even high-scale SUSY models.

2. $\Delta_{\rm HS}$

To include explicit dependence on the high-scale Λ at which the SUSY theory may be defined, we may write the *weak scale* parameters $m_{H_{u,d}}^2$ and μ^2 in Eq. (2) as

$$m_{H_{u,d}}^2 = m_{H_{u,d}}^2(\Lambda) + \delta m_{H_{u,d}}^2; \quad \mu^2 = \mu^2(\Lambda) + \delta\mu^2, \quad (6)$$

where $m_{H_{u,d}}^2(\Lambda)$ and $\mu^2(\Lambda)$ are the corresponding parameters renormalized at the high-scale Λ. It is the $\delta m_{H_{u,d}}^2$ terms that will contain the $\log\Lambda$ dependence emphasized in constructs of natural SUSY models [27–29]. In this way, we write

$$\frac{m_Z^2}{2} = \frac{(m_{H_d}^2(\Lambda) + \delta m_{H_d}^2 + \Sigma_d^d) - (m_{H_u}^2(\Lambda) + \delta m_{H_u}^2 + \Sigma_u^u)\tan^2\beta}{\tan^2\beta - 1} - (\mu^2(\Lambda) + \delta\mu^2). \quad (7)$$

In the same spirit used to construct $\Delta_{\rm EW}$, we can now define a fine-tuning measure that encodes the information about the high-scale origin of the parameters by requiring that each of the terms on the right-hand side of Eq. (7) (normalized again to $m_Z^2/2$) be smaller than a value $\Delta_{\rm HS}$. The high-scale fine-tuning measure $\Delta_{\rm HS}$ is thus defined to be

$$\Delta_{\rm HS} \equiv \max_i |B_i|/(m_Z^2/2), \quad (8)$$

with $B_{H_d} \equiv m_{H_d}^2(\Lambda)/(\tan^2\beta - 1)$ etc., defined analogously to the set C_i.

As discussed above, in models such as mSUGRA whose domain of validity extends to very high scales, because of the large logarithms one would expect that (barring seemingly accidental cancellations) the $B_{\delta H_u}$ contributions to

$\Delta_{\rm HS}$ would be much larger than any contributions to $\Delta_{\rm EW}$ because the term $m_{H_u}^2$ evolves from large m_0^2 through zero to negative values in order to radiatively break electroweak symmetry. Thus, $\Delta_{\rm HS}$ is numerically very similar to the EWFT measure advocated by Kitano-Nomura [27] where $\Delta_{\rm KN} = \delta m_{H_u}^2/(m_h^2/2)$.

Scans of the mSUGRA/CMSSM model in Ref. [30] found $\Delta_{\rm HS} \gtrsim 10^3$. In Ref. [25], scans over the NUHM2 model similarly found $\Delta_{\rm HS} \gtrsim 10^3$. Thus, both the mSUGRA and NUHM2 models would qualify as highly EW fine tuned under $\Delta_{\rm HS}$.

B. Goals of this paper

In this paper, we would like to maintain the SUSY grand desert scenario where the MSSM is postulated as the correct effective theory below $Q \simeq m_{\rm GUT}$. However, we would like to expand our set of input parameters, in this case, to a maximal set of 19, which maintains the scenario of minimal flavor and minimal CP violation. The resulting model, dubbed here as SUGRA19 [31], has the same parameter freedom as the more popular pMSSM model [32]. However, unlike pMSSM defined at the weak scale, SUGRA19 maintains the successes of renormalization group evolution and its consequent gauge coupling unification and radiative electroweak symmetry breaking due to the large value of m_t.

In this paper, we have several goals. The first is to check, under models with maximal parameter freedom, whether even lower values of $\Delta_{\rm EW} \ll 10$ can be found, or whether NUHM2 already achieves the minimal EWFT values. We will find that $\Delta_{\rm EW} \sim 5$–10 is about as low as can be achieved while maintaining accordance with phenomenological constraints, and that the resulting models tend to look phenomenologically rather similar to RNS models as derived from NUHM2 parameter space.

Our second goal is to check whether values of $\Delta_{\rm HS} \ll 10^3$ can be found. In the case of SUGRA19, we will find that $\Delta_{\rm HS}$ as low as 5–10 can also be found, but only for special choices of nonuniversal SUGRA parameters. The low $\Delta_{\rm HS}$ models appear tightly constrained if accordance with BF($b \to s\gamma$) measurements is imposed. Both the low $\Delta_{\rm EW}$ and the low $\Delta_{\rm HS}$ models are characterized by light Higgsinos with mass $\sim$100–300 GeV, which should be accessible to linear collider searches, although perhaps not accessible to LHC searches. We present some interesting benchmark (BM) points for both low $\Delta_{\rm EW}$ and low $\Delta_{\rm HS}$.

Before proceeding, we mention our results in relation to several previous works on reduced EWFT in models with nonuniversal soft SUSY breaking terms. After several initial studies using the BG measure in universal models [10–13,15], Kane and King [17] showed that nonuniversal gaugino masses with $M_1, M_2 > M_3$ lead to reduced EWFT. These were followed by similar studies by Lebedev *et al.* [19], Abe *et al.* [20], Martin [21] (the latter of which was used to motivate a compressed SUSY mass spectrum) and Antusch *et al.* [22]. Recently, Gogoladze *et al.* [33] studied the measures $\Delta_{\rm EW}$ and $\Delta_{\rm HS}$ within the context of Grand Unified Theory (GUT)-motivated gaugino mass nonuniversality using effectively a 5-parameter model with gaugino masses related by $M_1 = \frac{2}{5}M_3 + \frac{3}{5}M_2$. In their study, they were already able to reduce the maximum $\Delta_{\rm HS}$ values down to the $\sim$30 level, which is already quite close to what is achieved here using 19 free parameters.

II. SCAN OVER 19-PARAMETER SUGRA MODEL

To calculate superparticle mass spectra in the SUGRA19 model, we employ the Isajet 7.83 [34] SUSY spectrum generator Isasugra [35]. Isasugra begins the calculation of the sparticle mass spectrum with input $\overline{DR}$ gauge couplings and f_b, f_τ Yukawa couplings at the scale $Q = M_Z$ (f_t running begins at $Q = m_t$) and evolves the six couplings up in energy to the scale $Q = M_{\rm GUT}$ (defined as the value Q where $g_1 = g_2$) using two-loop renormalization group equations (RGEs). We do not enforce the exact unification condition $g_3 = g_1 = g_2$ at $M_{\rm GUT}$, since a few percent deviation from unification can be attributed to unknown GUT-scale threshold corrections [36]. Next, we impose the SSB boundary conditions at $Q = M_{\rm GUT}$ and evolve the set of 26 coupled two-loop MSSM RGEs [37,38] back down in scale to $Q = M_Z$. Full two-loop MSSM RGEs are used for soft term evolution, and the gauge and Yukawa coupling evolution includes threshold effects in the one-loop beta functions; thus, the gauge and Yukawa couplings transition smoothly from the MSSM to SM effective theories as different mass thresholds are passed. In Isasugra, the values of SSB terms which mix are frozen out at the scale $Q = m_{\rm SUSY} = \sqrt{m_{\tilde{t}_L} m_{\tilde{t}_R}}$, while nonmixing SSB terms are frozen out at their own mass scale [35]. The scalar potential is minimized using the RG-improved one-loop MSSM effective potential evaluated at an optimized scale $Q = m_{\rm SUSY}$ to account for leading two-loop effects [39]. Once the tree-level sparticle mass spectrum is obtained, one-loop radiative corrections are calculated for all sparticle and Higgs boson masses, including complete one-loop weak scale threshold corrections for the top, bottom and tau masses at scale $Q = m_{\rm SUSY}$ [40]. Since Yukawa couplings are modified by the threshold corrections, the solution must be obtained iteratively, with successive up-down running until a convergence at the required level is found.

We search for models with low $\Delta_{\rm EW}$ and low $\Delta_{\rm HS}$ by first performing a *broad-based* random scan over the following SUGRA19 parameter ranges:

(i) Gaugino masses: M_1, M_2, M_3: 0–3.5 TeV,
(ii) First and second generation scalar masses: m_{Q_1}, m_{U_1}, m_{D_1}, m_{L_1}, m_{E_1}: 0–3.5 TeV,
(iii) Third generation scalar masses: m_{Q_3}, m_{U_3}, m_{D_3}, m_{L_3}, m_{E_3}: 0–3.5 TeV,
(iv) Higgs soft masses: m_{H_u}, m_{H_d}: 0–3.5 TeV,
(v) Trilinear soft terms: A_t, A_b, A_τ: -3.5 TeV $\to$ 3.5 TeV,

(vi) Ratio of weak scale Higgs vevs $\tan\beta$: 2–60.

We adopt a common mass for first and second generation scalars so as to avoid the most stringent SUSY flavor changing neutral current constraints [41].

We require of our solutions that

(i) electroweak symmetry be radiatively broken,
(ii) the neutralino $\tilde{Z}_1$ is the lightest MSSM particle,
(iii) the light chargino mass obeys the model independent LEP2 limit, $m_{\tilde{W}_1} > 103.5$ GeV [42], and
(iv) $123 < m_h < 128$ GeV.

We do not impose any LHC sparticle search limits since our general scan can produce compressed spectra which in many cases can easily elude LHC gluino and squark searches. Points which satisfy the above constraints are plotted as blue circles in the following scatter plots (Fig. 1 and Figs. 4–14).

We will also calculate the values of BF($b \to s\gamma$) [43,44] and BF($B_S \to \mu^+\mu^-$) [45] for each point generated. The measured value of BF($b \to s\gamma$) is found to be $(3.55 \pm 0.26) \times 10^{-4}$ [46]. For comparison, the SM prediction [47] is $\mathrm{BF}^{\mathrm{SM}}(b \to s\gamma) = (3.15 \pm 0.23) \times 10^{-4}$. Also, recently the LHCb Collaboration has found an excess over the background for the decay $B_s \to \mu^+\mu^-$ [48]. They find a branching fraction of $\mathrm{BF}(B_s \to \mu^+\mu^-) = 3.2^{+1.5}_{-1.2} \times 10^{-9}$ which is in accordance with the SM prediction of $(3.2 \pm 0.2) \times 10^{-9}$. Points with BF($b \to s\gamma$) within 3σ of its measured value $\mathrm{BF}(b \to s\gamma) = (2.5\text{–}4.5) \times 10^{-4}$ and points with $\mathrm{BF}(B_s \to \mu^+\mu^-) = (2\text{–}4.7) \times 10^{-9}$ will be labeled as light blue, showing that these points are also in accordance with B-physics constraints.

Our first set of results is shown in Fig. 1. The broad scan points are shown in blue. We see that the bulk of generated points yield Δ_{EW} and $\Delta_{\mathrm{HS}} \gtrsim 10^3$, so would qualify as highly EW fine tuned in generating $m_Z = 91.2$ GeV. The points with the lowest Δ_{EW} values come in with $\Delta_{\mathrm{EW}} \sim 10$, which is similar to that which can be achieved in the more restrictive NUHM2, but which is much better than what can be achieved in mSUGRA.

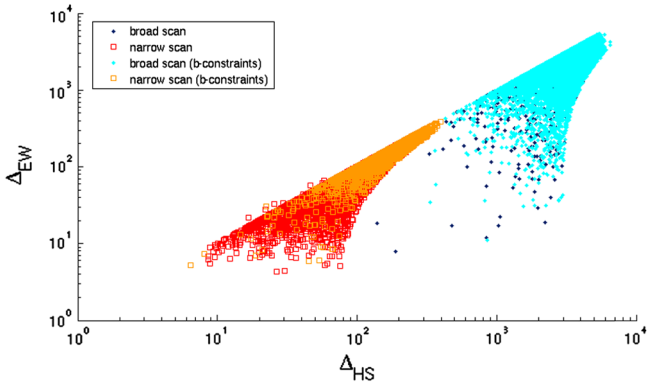

FIG. 1 (color online). Plot of Δ_{HS} vs Δ_{EW} from a broad (dark/light blue) and focused (red/orange) scan over SUGRA19 model parameter space. The orange and light blue points satisfy B-decay constraints, while the dark blue and red points do not.

The lowest Δ_{EW} point has $\Delta_{\mathrm{EW}} = 7.9$, while the corresponding $\Delta_{\mathrm{HS}} = 190$. The SUGRA19 parameters associated with this point are listed in Table I in the column labeled as EW1. The point has the required low $\mu \sim 180$ GeV and $m^2_{H_u}(m_{\mathrm{weak}}) \sim -(171\ \mathrm{GeV})^2$. In addition, the large top-squark mixing $A_t/m_Q(3) \sim -2.1$ softens the top-squark radiative corrections $\Sigma^u_u(\tilde{t}_{1,2})$ while raising m_h up to 123.5 GeV.

The corresponding sparticle mass spectra are listed in Table II. The gluinos and squarks are ~2–3 TeV: well beyond the current LHC reach. The $\tilde{W}^{\pm}_2$ and $\tilde{Z}_{1,2}$ are dominantly Higgsino-like with a mass gap $m_{\tilde{Z}_2} - m_{\tilde{Z}_1} \simeq 3$ GeV. Thus, even though the Higgsinos can be produced with large cross sections at the LHC, the very soft visible energy release from their decays makes them difficult to detect [49]. The light Higgsinos should be straightforward to detect at a linear e^+e^- collider with $\sqrt{s} \gtrsim 400$ GeV. The lightest top squark $\tilde{t}_1$ has mass less than 1 TeV: typically below values generated from radiative natural SUSY models [25]. This leads to a somewhat anomalous branching fraction $\mathrm{BF}(b \to s\gamma) \sim 2.5 \times 10^{-4}$, below the measured value of $(3.55 \pm 0.26) \times 10^{-4}$ [46].

A perhaps surprising result from Fig. 1 is that Δ_{HS} values far below the NUHM2/mSUGRA minimal value of 10^3 can now be found. In fact, the lowest Δ_{HS} point from the broad scan has a value of 32, or 3.1% EWFT, even including the effect of high-scale logarithms. The parameter values for

TABLE I. Input parameters (GUT scale) in GeV for one low Δ_{EW} point and two low Δ_{HS} points. We take $m_t = 173.2$ GeV.

Parameter	EW1	HS1	HS2
$M_1(m_{\mathrm{GUT}})$	2822.1	3266.2	3416.4
$M_2(m_{\mathrm{GUT}})$	3385.3	2917.8	3091.3
$M_3(m_{\mathrm{GUT}})$	884.9	1095.7	1085.8
$m_Q(1)$	2484.7	1192.6	978.5
$m_U(1)$	2506.2	2468.3	2440.6
$m_D(1)$	2342.1	1508.9	1404.2
$m_L(1)$	1820.4	623.8	754.8
$m_E(1)$	1731.2	936.1	915.8
$m_Q(3)$	698.3	6.6	371.3
$m_U(3)$	1552.8	233.9	23.2
$m_D(3)$	1498.5	2946.0	3052.4
$m_L(3)$	3339.3	341.1	451.3
$m_E(3)$	2114.9	1268.7	1247.5
m_{H_u}	871.3	314.0	125.4
m_{H_d}	2205.3	3160.4	2964.9
A_t	−1509.6	−1024.4	−801.3
A_b	2301.7	3121.6	3294.3
A_τ	3307.3	1932.0	1754.5
$\tan\beta$	27.0	51.1	29.0
μ	181.4	242.8	98.0
Δ_{EW}	7.9	17.9	5.2
Δ_{HS}	190.0	32.0	6.4

TABLE II. Sparticle masses in GeV and observables for one low $\Delta_{\rm EW}$ and two low $\Delta_{\rm HS}$ points as in Table I. The measured values of the branching fractions are $\mathrm{BF}(b \to s\gamma) = (3.55 \pm 0.26) \times 10^{-4}$ and $\mathrm{BF}(B_s \to \mu^+\mu^-) = 3.2^{+1.5}_{-1.2} \times 10^{-9}$.

Mass (GeV)	EW1	HS1	HS2
$m_{\tilde{g}}$	2042.9	2436.7	2428.8
$m_{\tilde{u}_L}$	3650.7	2991.9	2968.5
$m_{\tilde{u}_R}$	2980.5	3214.8	3191.6
$m_{\tilde{e}_R}$	2196.3	1763.6	1786.1
$m_{\tilde{t}_1}$	879.5	1033.2	892.4
$m_{\tilde{t}_2}$	2305.1	1958.3	2394.9
$m_{\tilde{b}_1}$	2121.8	1961.4	2418.0
$m_{\tilde{b}_2}$	2327.7	2916.1	3495.8
$m_{\tilde{\tau}_1}$	2219.6	1049.5	1748.3
$m_{\tilde{\tau}_2}$	3865.8	1467.5	1911.3
$m_{\tilde{\nu}_\tau}$	3884.8	1464.9	1911.4
$m_{\tilde{W}_2}$	2802.2	2393.0	2538.3
$m_{\tilde{W}_1}$	192.1	255.5	104.1
$m_{\tilde{Z}_4}$	2810.2	2386.8	2530.3
$m_{\tilde{Z}_3}$	1261.2	1448.0	1513.5
$m_{\tilde{Z}_2}$	187.8	251.2	102.4
$m_{\tilde{Z}_1}$	184.7	247.9	99.3
m_A	2759.7	2242.6	3176.4
m_h	123.5	123.6	123.1
$\Omega^{\rm std}_{\tilde{Z}_1}h^2$	0.007	0.013	0.003
$\mathrm{BF}(b \to s\gamma) \times 10^4$	2.5	1.8	2.6
$\mathrm{BF}(B_s \to \mu^+\mu^-) \times 10^9$	3.9	4.5	3.8
$\sigma^{\rm SI}(\tilde{Z}_1 p)$ (pb)	2.9×10^{-10}	3.7×10^{-10}	2.5×10^{-10}

this point, labeled as HS1, are also listed in Table I. There are several features of the input parameters which lead to low $\Delta_{\rm HS}$. First, the GUT scale value of $m^2_{H_u} = (314\ \mathrm{GeV})^2$, so our high-scale starting point for m_{H_u} is not too far from m_Z. Second, the GUT scale gaugino masses M_1 and M_2 are $\sim 3M_3 \sim 3$ TeV. The RG running of $m^2_{H_u}$ is governed by

$$\frac{dm^2_{H_u}}{dt} = \frac{2}{16\pi^2}\left(-\frac{3}{5}g_1^2M_1^2 - 3g_2^2M_2^2 + \frac{3}{10}g_1^2S + 3f_t^2X_t\right) \tag{9}$$

where $t = \log(Q^2/\mu^2)$, $S = m^2_{H_u} - m^2_{H_d} + \mathrm{Tr}[\mathbf{m}^2_Q - \mathbf{m}^2_L - 2\mathbf{m}^2_U + \mathbf{m}^2_D + \mathbf{m}^2_E]$ and $X_t = m^2_Q(3) + m^2_U(3) + m^2_{H_u} + A_t^2$. At $Q = m_{\rm GUT}$, the large gaugino masses provide a large negative slope (green curve of Fig. 2) for $m^2_{H_u}$, causing its value to increase while running towards lower mass scales. As the parameters evolve, X_t increases due to the increasing squark soft terms so that the Yukawa coupling term grows (red curve from Fig. 2) and ultimately dominates; then $m^2_{H_u}$ is driven towards negative values, so that electroweak symmetry is finally broken. The total slope (black curve) passes through zero around $Q \sim 10^{10}$ GeV, indicating large cancellations in the RG running of $m^2_{H_u}$. Ultimately, the value of $m^2_{H_u}(m_{\rm weak}) \sim -(185\ \mathrm{GeV})^2$ so

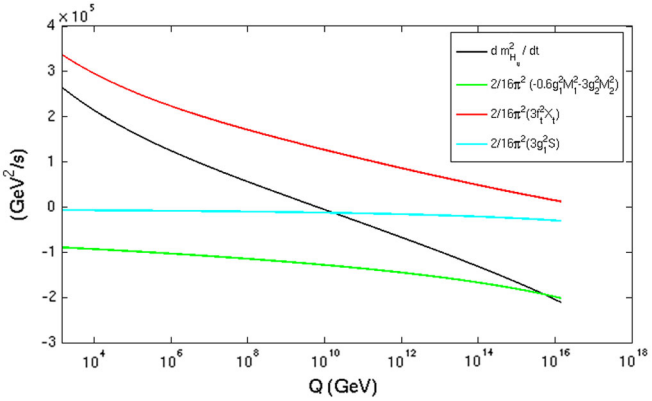

FIG. 2 (color online). Plot of slope $dm^2_{H_u}/dt$ vs Q from model HS1 with $\Delta_{\rm HS} = 32$.

that both the starting and ending points of $m^2_{H_u}$ remain not too far from m^2_Z, and hence $\delta m^2_{H_u}$ is not too far from m^2_Z, thus fulfilling the most important condition required by low $\Delta_{\rm HS}$.

The RG running of gaugino masses and selected soft scalar masses for HS1 are shown in Fig. 3. In frame (a), we see that indeed M_1 and M_2 start at $\sim$3 TeV values and decrease, while M_3 starts small at $Q = m_{\rm GUT}$ and sharply increases. The gaugino mass boundary conditions then influence the running of the soft scalar masses in frame (b).

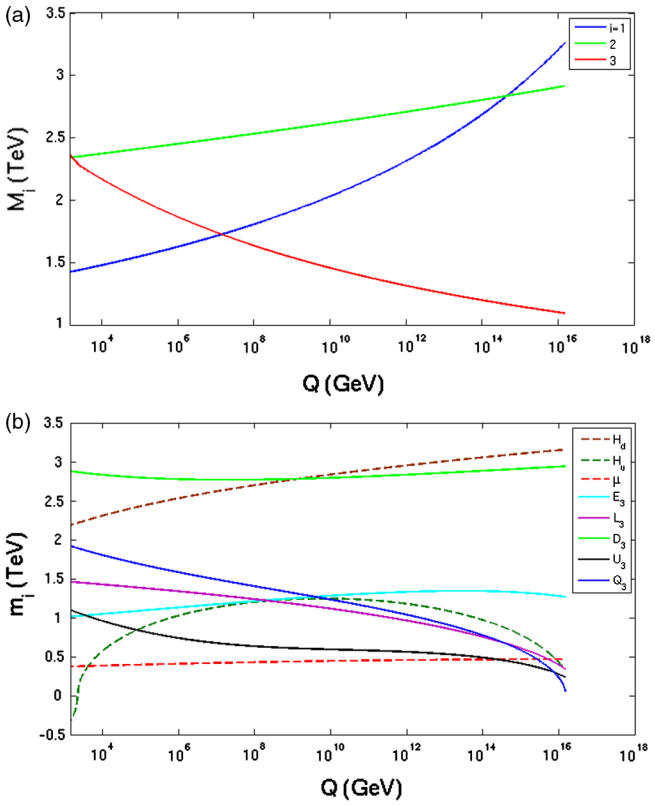

FIG. 3 (color online). Plot of (a) running gaugino masses and (b) running scalar masses vs Q from model HS1 with $\Delta_{\rm HS} = 32$.

Most important is the running of $m_{H_u}^2$, which starts near m_Z^2 at $m_{\rm GUT}$, runs up to about the TeV scale at $Q \sim 10^{10}$ GeV, and then is pushed to small negative values by $Q \sim m_{\rm weak}$. Also, $m_U(3)$ and $m_Q(3)$ start small, which aides the high Q gaugino dominance in the running of $m_{H_u}^2$. By $Q \sim m_{\rm weak}$, these third generation squark soft terms have been pushed to the TeV scale. Thus, top squarks are not so heavy and the radiative corrections $\Sigma_u^u(\tilde{t}_{1,2})$ are under control.

III. RESULTS FROM NARROW SCAN

To hone in on SUGRA19 solutions with low $\Delta_{\rm HS}$, we will impose a narrow, dedicated scan about our lowest $\Delta_{\rm HS}$ solution:

(i) M_1: 3–3.5 TeV, M_2: 2.7–3.2 TeV, M_3: 0.8–1.3 TeV,
(ii) $m_Q(1,2)$: 0.9–1.4 TeV, $m_U(1,2)$: 2.2–2.7 TeV, $m_D(1,2)$: 1.25–1.75 TeV, $m_L(1,2)$: 0.4–0.9 TeV, $m_E(1,2)$: 0.7–1.2 TeV,
(iii) $m_Q(3)$: 0–0.5 TeV, $m_U(3)$: 0–0.5 TeV, $m_D(3)$: 2.7–3.2 TeV, $m_L(3)$: 0.1–0.5 TeV, $m_E(3)$: 1–2 TeV,
(iv) m_{H_u}: 0.05–0.55 TeV, m_{H_d}: 2.9–3.4 TeV,
(v) A_t: $-1.3 \to -0.8$ TeV, A_b: 2.9–3.4 TeV, A_τ: 1.7–2.2 TeV,

with $\tan\beta$ still 2–60 as before.

A. SUGRA19 parameters for low $\Delta_{\rm HS}$ solutions

The results from our narrow scan are shown in Fig. 1 as red xs, while points that obey B-constraints are labeled as orange xs. The more focused sampling over lucrative parameter ranges has produced points with much lower $\Delta_{\rm EW}$ values ranging down to ~5, and also solutions with $\Delta_{\rm HS}$ as low as 6. The $\Delta_{\rm HS} = 6.4$ solution is presented in Tables I and II as the BM model HS2. While point HS2 has μ of just 98 GeV, the lightest chargino mass is $m_{\tilde{W}_1} = 104.1$ GeV, slightly beyond the limit from LEP2 searches. Since gluino and squark masses are in the several TeV range, the point is also safe from LHC8 searches. The mass gaps $m_{\tilde{W}_1} - m_{\tilde{Z}_1} = 4.8$ GeV and $m_{\tilde{Z}_2} - m_{\tilde{Z}_1} = 3.1$ GeV, so again there will be only a tiny visible energy release from the Higgsino decays.

To display the sort of parameter choices leading to low $\Delta_{\rm HS}$, we show in Fig. 4 the values of $\Delta_{\rm EW}$ (blue points) and $\Delta_{\rm HS}$ (red/orange points) versus superpotential Higgsino mass μ from the broad (circles) and narrow (x's) scan. From the plot, we see unambiguously that low $|\mu| \sim m_Z$ is a necessary, but not sufficient, condition to obtain *both* low $\Delta_{\rm EW}$ and low $\Delta_{\rm HS}$. This translates into the solid prediction that four light Higgsinos should lie within reach of a linear e^+e^- collider with $\sqrt{s} > 2|\mu|$.

In Fig. 5, we show $\Delta_{\rm HS}$ and $\Delta_{\rm EW}$ vs $m_{H_u}(m_{\rm GUT})$ from the broad and narrow scans over SUGRA19 parameter space. Here, we see that low $\Delta_{\rm EW}$ solutions can be obtained over a large range of $m_{H_u}(m_{\rm GUT})$ values, as expected from radiative natural SUSY results [25] which allow for a large

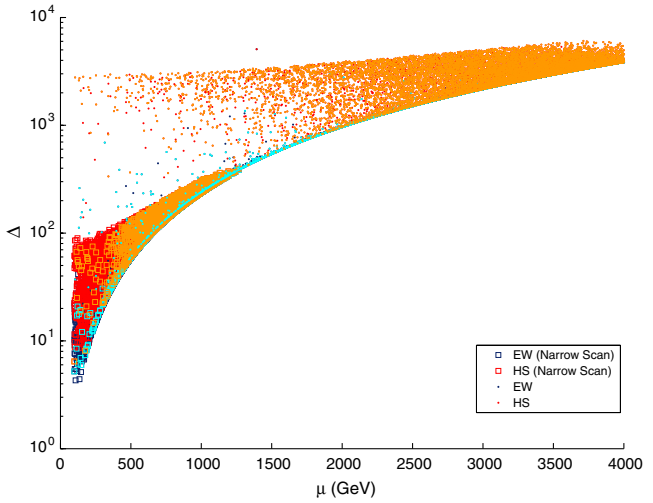

FIG. 4 (color online). Plot of $\Delta_{\rm HS}$ and $\Delta_{\rm EW}$ vs μ from the scan over SUGRA19 model parameter space. Color coding is the same as in Fig. 1.

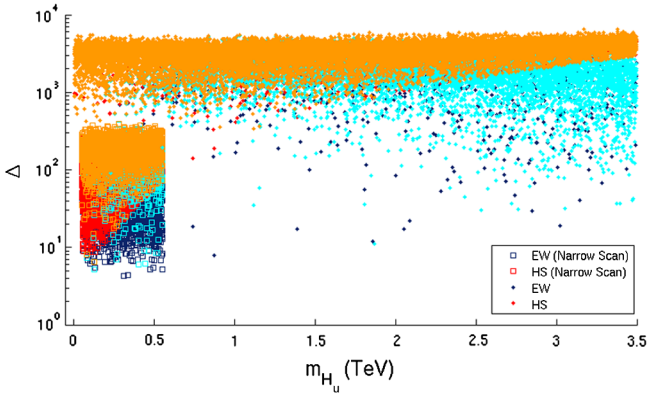

FIG. 5 (color online). Plot of $\Delta_{\rm HS}$ and $\Delta_{\rm EW}$ vs $m_{H_u}(m_{\rm GUT})$ from the scan over SUGRA19 model parameter space. Color coding is the same as in Fig. 1.

cancellation between $m_{H_u}^2(m_{\rm GUT})$ and $\delta m_{H_u}^2$. However, the low $\Delta_{\rm HS}$ solutions are only obtained for $m_{H_u}(m_{\rm GUT})$ not too far from m_Z, as required by Eq. (7).

In Fig. 6, we show $\Delta_{\rm HS}$ and $\Delta_{\rm EW}$ vs M_3, where we note that $m_{\tilde{g}} \simeq |M_3|$ up to radiative corrections. Low $\Delta_{\rm EW}$ values allow for $M_3 \sim 1$–3 TeV, in accordance with LHC searches which require $m_{\tilde{g}} \gtrsim 1$ TeV for not-too-compressed spectra.

In the two frames of Fig. 7, we show $\Delta_{\rm HS}$ and $\Delta_{\rm EW}$ vs (a) M_1/M_3 and (b) M_2/M_3, where all gaugino masses are GUT scale values. The narrow scan has focused on the region around $M_3 \sim 1$ TeV, where solutions with $\Delta_{\rm HS} \lesssim 10$–100 can be found. From both frames, we see that nonuniversal GUT scale gaugino masses are required for low $\Delta_{\rm HS}$ solutions, with ratios in the range M_1/M_3 and $M_2/M_3 \sim 2$–4 being preferred. As remarked earlier, the large electroweak gaugino masses provide an initial upwards evolution of $m_{H_u}^2$

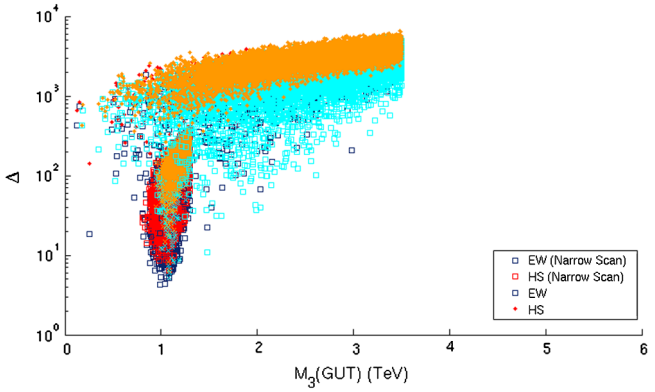

FIG. 6 (color online). Plot of $\Delta_{\rm HS}$ and $\Delta_{\rm EW}$ vs M_3 ($\sim m_{\tilde{g}}$) from the scan over SUGRA19 model parameter space. Color coding is the same as in Fig. 1.

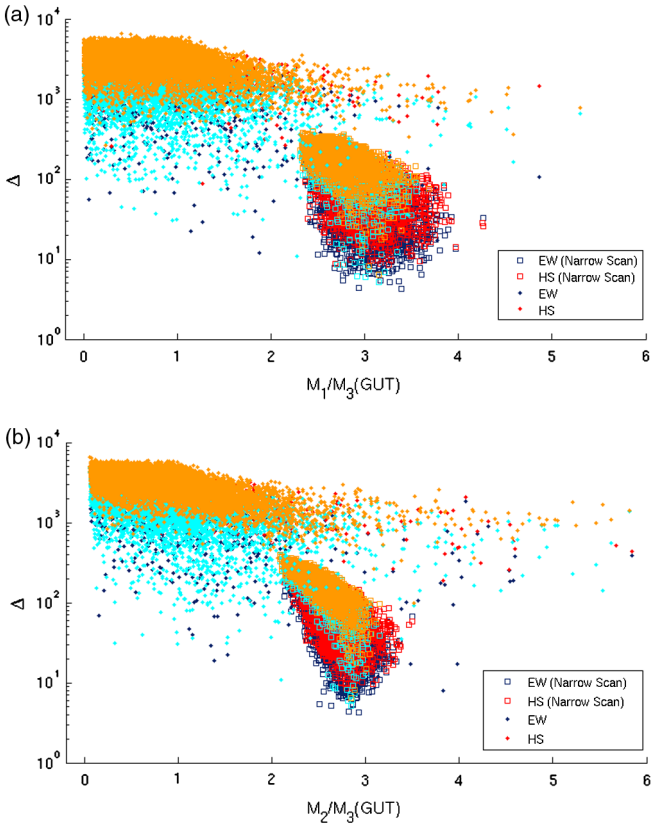

FIG. 7 (color online). Plot of $\Delta_{\rm HS}$ and $\Delta_{\rm EW}$ vs (a) M_1/M_3 and (b) M_2/M_3 from the scan over SUGRA19 model parameter space. Color coding is the same as in Fig. 1.

which is later canceled by the downward push from the top Yukawa coupling at lower Q values.

B. Sparticle mass spectra from low $\Delta_{\rm HS}$ solutions

We have already seen from Fig. 4 that very low values of $\mu \sim 100$–300 GeV are required for both low $\Delta_{\rm HS}$ and low $\Delta_{\rm EW}$ solutions. This translates into the requirement of four light Higgsino states $\tilde{W}_1^{\pm}$ and $\tilde{Z}_{1,2}$ with mass

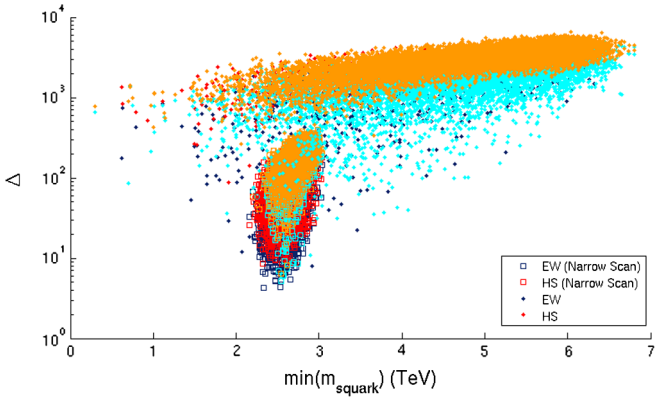

FIG. 8 (color online). Plot of $\Delta_{\rm HS}$ and $\Delta_{\rm EW}$ vs min($m_{\tilde{q}}$) from scans over SUGRA19 model parameter space. Color coding is the same as in Fig. 1.

$\sim$100–300 GeV, which are difficult to observe at the LHC but should be observable at a linear e^+e^- collider.

What of gluinos and squarks? We have already seen that $m_{\tilde{g}} \sim 1$–3 TeV is allowed for low $\Delta_{\rm EW}$ solutions, while low $\Delta_{\rm HS}$ solutions prefer a lower value $m_{\tilde{g}} \sim 1$ TeV. This is due to the fact that too large a value of $M_3(m_{\rm GUT})$ (and hence a larger physical gluino mass) would cause an increase in third generation squark masses, which would increase the X_t factor in the $m_{H_u}^2$ RGE and cause a larger value of $\delta m_{H_u}^2$ to ensue.

In Fig. 8, we show $\Delta_{\rm HS}$ and $\Delta_{\rm EW}$ values versus min$[m_{\tilde{q}}]$, where the min is over all physical squark masses of the first two generations. While low $\Delta_{\rm EW}$ solutions allow for a broad range of $m_{\tilde{q}} \sim 1$–5 TeV, the low $\Delta_{\rm HS}$ solutions tend to favor $m_{\tilde{q}} \sim 2$–3 TeV, beyond the current LHC reach.

In Fig. 9, we show $\Delta_{\rm HS}$ and $\Delta_{\rm EW}$ versus top-squark masses (a) $m_{\tilde{t}_1}$ and (b) $m_{\tilde{t}_2}$. The lowest $\Delta_{\rm HS}$ solutions are found for $m_{\tilde{t}_1} \sim 1$ TeV and $m_{\tilde{t}_2} \sim 2$ TeV. These values are typically 1–2 TeV lower than results from RNS models but still beyond most LHC reach projections for third generation squark detection. The lowest $\Delta_{\rm HS}$ solutions, colored dark blue and red, are usually in violation of the B-constraints. This reflects the fact that low $\Delta_{\rm HS}$ requires light Higgsino-like charginos (low μ) and light stops, and hence there tend to be large anomalous contributions to the BF($b \to s\gamma$) branching fraction.

In Fig. 10, we show $\Delta_{\rm HS}$ and $\Delta_{\rm EW}$ vs m_A. Here, we see that the lowest Δ solutions favor m_A (and hence m_H and $m_{H^\pm}$) in the 2–4 TeV range, usually well beyond any projected LHC or ILC reach.

C. Low $\Delta_{\rm HS}$ solutions and B-physics constraints

1. BF($B_s \to \mu^+\mu^-$)

In Fig. 11, we show values of $\Delta_{\rm EW}$ and $\Delta_{\rm HS}$ vs BF($B_s \to \mu^+\mu^-$). The recent LHCb measurement [48] finds the branching fraction of BF($B_s \to \mu^+\mu^-$) $= 3.2^{+1.5}_{-1.2} \times 10^{-9}$, in accordance with the SM prediction of $(3.2 \pm 0.2) \times 10^{-9}$.

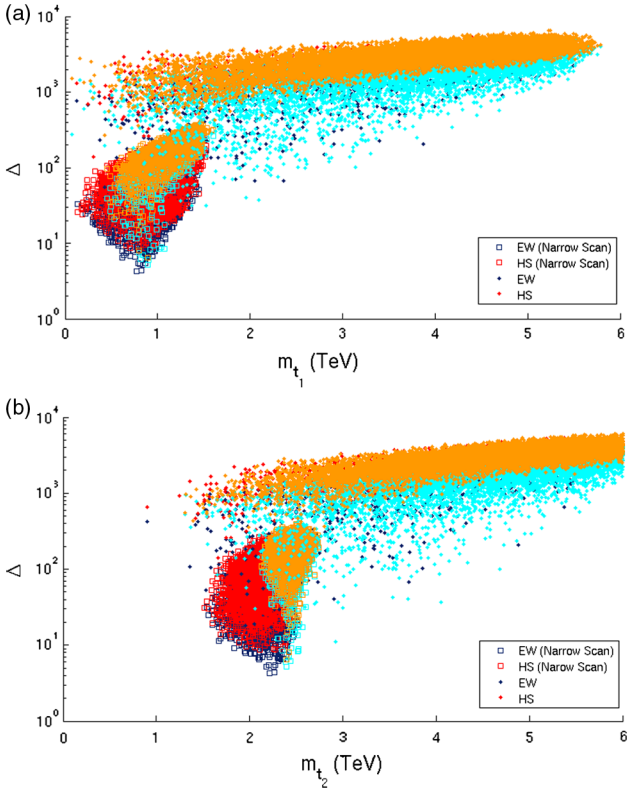

FIG. 9 (color online). Plot of $\Delta_{\rm HS}$ and $\Delta_{\rm EW}$ vs (a) $m_{\tilde{t}_1}$ and (b) $m_{\tilde{t}_2}$ from scans over SUGRA19 model parameter space. Color coding is the same as in Fig. 1.

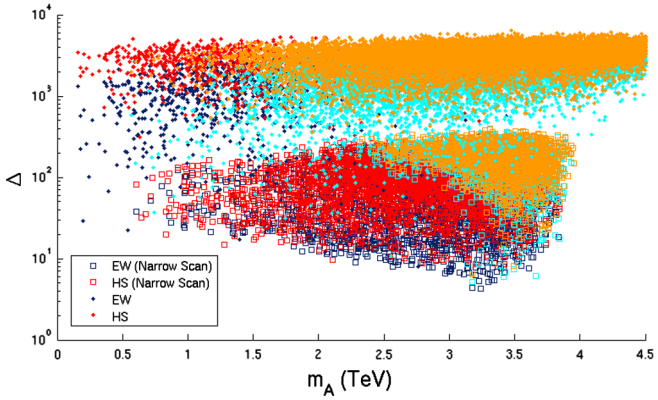

FIG. 10 (color online). Plot of $\Delta_{\rm HS}$ and $\Delta_{\rm EW}$ vs m_A from scans over SUGRA19 model parameter space. Color coding is the same as in Fig. 1.

In supersymmetric models, this flavor-changing decay occurs through pseudoscalar Higgs A exchange [45], and the contribution to the branching fraction from SUSY is proportional to $\frac{(\tan\beta)^6}{m_A^4}$. The decay is most constraining at large $\tan\beta$ and at low m_A. In the case of low $\Delta_{\rm HS}$ solutions with lower $\tan\beta$ and heavier m_A, we find the bulk of solutions to lie within the newly measured error bars, although some solutions with large $\Delta_{\rm HS}$ and $\Delta_{\rm EW}$ will be excluded.

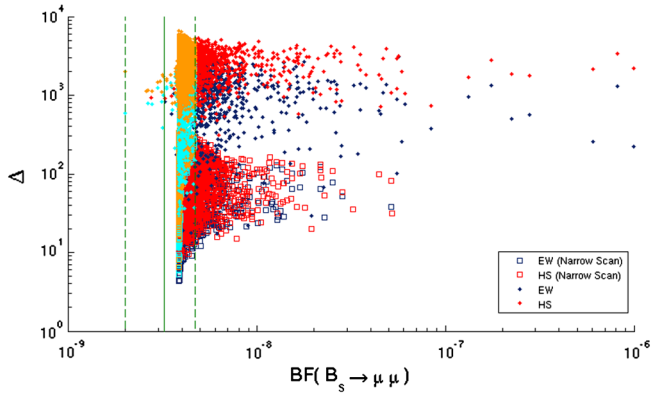

FIG. 11 (color online). Plot of $\Delta_{\rm EW}$ and $\Delta_{\rm HS}$ vs BF($B_s \to \mu^+\mu^-$) from a 19-parameter scan. Color coding is the same as in Fig. 1. The vertical solid line is the measured value, and the dashed lines are the 1σ uncertainties.

2. BF($b \to s\gamma$)

In Fig. 12, we show $\Delta_{\rm EW}$ and $\Delta_{\rm HS}$ vs BF($b \to s\gamma$). We also show the measured central value and both 1σ and 3σ error bars. SUSY contributions to the $b \to s\gamma$ decay rate come mainly from chargino-stop loops and the W-charged Higgs loops, and so are large when these particles are light and when $\tan\beta$ is large [43,44]. In the case shown here, where the low $\Delta_{\rm HS}$ solutions require third generation squarks somewhat heavier than generic natural SUSY but somewhat lighter than radiative natural SUSY, we find the bulk of low $\Delta_{\rm HS}$ solutions to lie a couple standard deviations below the measured value.

3. BF($B_u \to \tau^+\nu_\tau$)

The branching fraction for $B_u \to \tau^+\nu_\tau$ decay is calculated [50] in the SM to be BF($B_u \to \tau^+\nu_\tau$) $= (1.10 \pm 0.29) \times 10^{-4}$. This is to be compared to the value from the HFAG [51], which finds a measured value of BF($B_u \to \tau^+\nu_\tau$) $= (1.67 \pm 0.3) \times 10^{-4}$, somewhat beyond—but not

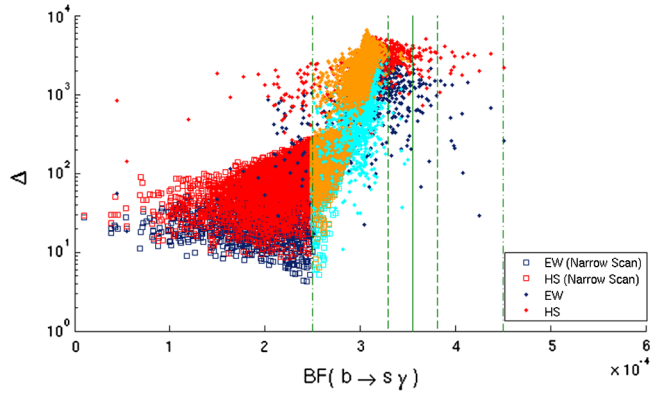

FIG. 12 (color online). Plot of $\Delta_{\rm EW}$ and $\Delta_{\rm HS}$ vs BF($b \to s\gamma$) from a 19-parameter scan. Color coding is the same as in Fig. 1. The vertical solid line is the measured value, and the dashed lines are the 1σ and 3σ uncertainties.

in disagreement with—the SM prediction. The main contribution from SUSY arises due to tree-level charged Higgs exchange, and is large at large tan β and low m_{H^+}. In Fig. 13, we plot the expected branching fraction BF($B_u \to \tau^+ \nu_\tau$) vs $\Delta_{\rm EW}$ and $\Delta_{\rm HS}$. Here, we see that the SUSY prediction tends to cluster around the SM predicted value, with some deviations for lower branching fractions.

4. BF($\bar{B} \to D^{(*)} \tau^- \bar{\nu}_\tau$)

Recently, the *BABAR* Collaboration [52] has measured an excess of $\bar{B} \to D\tau^- \bar{\nu}_\tau$ events compared to $\bar{B} \to D\ell^- \bar{\nu}_\ell$ (where $\ell = e$ or μ) at 2σ and an excess of $\bar{B} \to D^* \tau^- \bar{\nu}_\tau$ at 2.7σ. The combined deviation is a 3.4σ effect. Such a deviation can occur in SUSY models mainly due to decay through a charged Higgs H^-, but m_{H^-} would have to be well below the LEP2 limit [52]. In our SUGRA19 scans, $m_{H^\pm} \simeq m_A \sim$ 2–4 TeV. Thus, we would expect little deviation from the SM prediction for our SUSY scenario.

5. $R_b \equiv \Gamma(Z \to b\bar{b})/\Gamma(Z \to$ ***hadrons***$)$

The branching fraction for $Z \to b\bar{b}$ compared to BF($Z \to$ hadrons) (R_b) has been measured to be $R_b = 0.21629 \pm 0.00066$ [53]. In contrast, a recent two-loop SM calculation [54] finds $R_b \simeq 0.2149$, which provides a $\sim 2\sigma$ discrepancy. In SUSY models, $Z \to b\bar{b}$ depends also on $\tilde{t}_{1,2}\tilde{W}_{1,2}$ and $\tilde{b}_i\tilde{Z}_j$ loop corrections [55]. To explain such a deviation using SUSY, theory estimates seem to require top squarks and charginos below the LEP2 bounds [56,57]. For the SUGRA19 scans presented here, with $m_{\tilde{t}_1} \sim$ 0.5–1.5 TeV, we expect nearly the SM value of R_b to be obtained.

D. Low $\Delta_{\rm HS}$ solutions and dark matter

In this section, we show values of the relic neutralino abundance from our scan over SUGRA19 parameter space. We use the IsaReD [58] relic density calculator from Isajet.

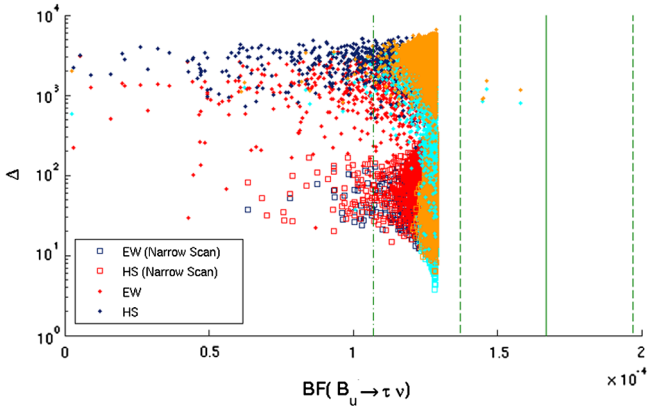

FIG. 13 (color online). Plot of $\Delta_{\rm EW}$ and $\Delta_{\rm HS}$ vs BF($B_u \to \tau\nu_\tau$) from a 19-parameter scan. Color coding is the same as in Fig. 1. The vertical solid line is the measured value, and the dashed lines are the 1σ and 2σ uncertainties.

Our results are shown in Fig. 14 frame (a), where we plot $\Delta_{\rm HS}$ and $\Delta_{\rm EW}$ vs $\Omega_{\tilde{Z}_1} h^2$. For comparison, we also show the location of the Planck-measured [59] relic density of dark matter (green dashed line). Both the low $\Delta_{\rm HS}$ and $\Delta_{\rm EW}$ solutions populate a band located well below the measured abundance. This reflects the fact that the low $\Delta_{\rm HS,EW}$ solutions all have low μ so that the $\tilde{Z}_1$ is dominantly Higgsino-like; these solutions enjoy an ample annihilation cross section into WW, ZZ etc. in the early universe. Thus, the lowest $\Delta_{\rm HS,EW}$ solutions are typically suppressed by factors of 10–50 below the measured dark matter abundance. Clearly, additional physics is needed in the early universe to gain accordance with experiment. One suggestion—the presence of late-decaying scalar fields—can either augment or diminish the relic abundance from its standard value [60]. Another possibility—mixed neutralino plus axion dark matter—is favored by SUSY models with a standard underabundance of neutralinos since thermal production of axinos and thermal/nonthermal production of saxions followed by decays to SUSY particles can augment the neutralino abundance [61] (depending on

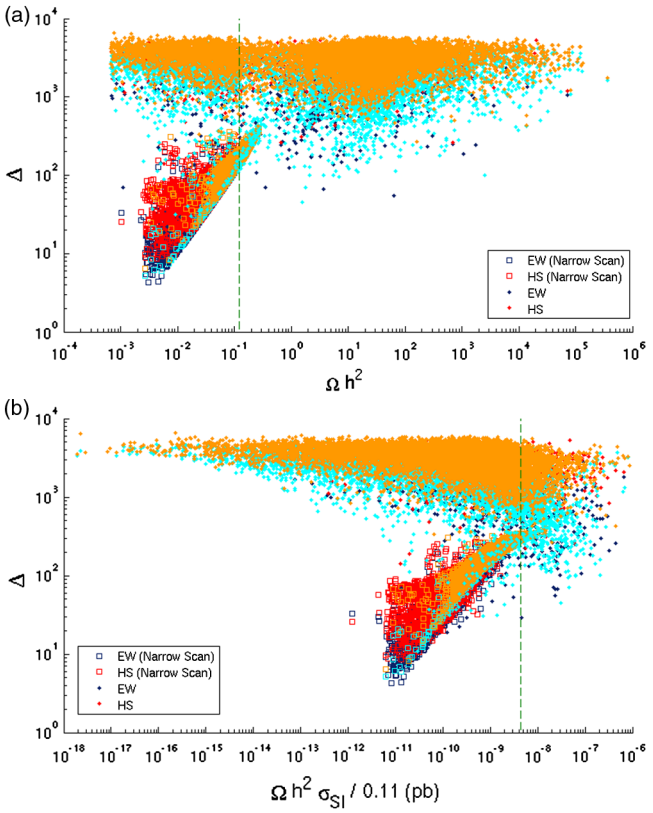

FIG. 14 (color online). Plot of $\Delta_{\rm EW}$ and $\Delta_{\rm HS}$ vs (a) standard neutralino relic abundance $\Omega^{std}_{\tilde{Z}_1} h^2$ and (b) rescaled spin-independent $\sigma(\tilde{Z}_1 p)$ from a 19-parameter scan. Color coding is the same as in Fig. 1. The vertical dashed line in (a) is the Planck measured value, while in (b) it is the recent Xe-100 upper limit on spin-independent neutralino-proton scattering for a 150 GeV weakly interacting massive particle.

additional Peccei-Quinn parameters and the reheat temperature T_R after inflation). Any remaining gap in the generated neutralino abundance relative to the measured abundance can be made up of axions.

In Fig. 14(b), we plot the rescaled spin-independent neutralino-proton scattering cross section $(\Omega_{\tilde{Z}_1}^{\rm std}h^2/0.11)\,\sigma^{\rm SI}(\tilde{Z}_1 p)$ from IsaReS [62]. The prefactor accounts for the possibility that the local dark matter abundance may be well below the value assumed from neutralino-only cold dark matter (CDM). For reference, we show the latest Xe-100 limit [63] (dashed green line) for $m_{\tilde{Z}_1} = 150$ GeV. The rescaled direct detection (DD) cross section is below current sensitivity by 1–2 orders of magnitude. This is lower than even DD projections from radiative natural SUSY [64] since in that case the $\tilde{Z}_1$ is mainly Higgsino but with a non-negligible gaugino component. Since the $\tilde{Z}_1 - \tilde{Z}_1 - h$ coupling depends on a product of gaugino-Higgsino components, the value of $\sigma^{\rm SI}(\tilde{Z}_1 p)$ in the RNS case never gets too small. In our current case, with nonuniversal gaugino masses, the $\tilde{Z}_1$ can be a much more pure Higgsino state, and consequently can have a significantly lower DD rate.

IV. CONCLUSIONS

In previous studies, the radiative natural SUSY model has emerged as a way to reconcile low EWFT with a lack of SUSY signals at LHC8 and the presence of a light Higgs scalar with mass $m_h \sim 125$ GeV. The RNS model cannot be realized within the restrictive mSUGRA/CMSSM framework, but can be realized within the context of NUHM2 models (which depend on six input parameters) and where μ can be a free input value. In RNS models, $\Delta_{\rm EW}$ as low as $\sim$10 can be generated while $\Delta_{\rm HS}$ as low as 10^3 can be found.

In this study, we have implemented scans over the most general minimal flavor-violating and minimal *CP*-violating GUT scale SUSY model—SUGRA19—with two goals in mind. Our first goal was to check if the additional freedom of 13 extra parameters allows for much lower $\Delta_{\rm EW}$ solutions. In previous work—by proceeding from mSUGRA to NUHM2 models—a reduction in the minimum of $\Delta_{\rm EW}$ of at least a factor of 10 was found [25,30]. In the present work, we do not find any substantial reduction in the minimal $\Delta_{\rm EW}$ value by proceeding from the NUHM2 model to SUGRA19. The parameter freedom of NUHM2 appears sufficient to minimize $\Delta_{\rm EW}$ to its lowest values of $\sim$5–10.

Our second goal was to check whether the additional parameter freedom can improve on the high-scale EWFT parameter $\Delta_{\rm HS}$. In this regard, we find improvements by factors ranging up to $\sim$150. In order to generate low values of $\Delta_{\rm HS}$, one must generate $\mu \sim 100$–300 GeV as usual, but also one must start with $m_{H_u}^2 \sim m_Z^2$ at the GUT scale, and then generate relatively little change in $\delta m_{H_u}^2$ during evolution from $m_{\rm GUT}$ to $m_{\rm weak}$. Small values of $\delta m_{H_u}^2$ can be found if one begins with electroweak gaugino masses $M_{1,2} \sim 3M_3$ at the GUT scale so that gaugino-induced RG evolution dominates at high $Q \sim m_{\rm GUT}$. Then at lower Q values approaching the weak scale, top-Yukawa terms dominate the running of $m_{H_u}^2$, leading to broken electroweak symmetry, but also leading to not much net change in $m_{H_u}^2$ during its evolution from $m_{\rm GUT}$ to $m_{\rm weak}$.

The solutions with low $\Delta_{\rm HS}$ are characterized by the presence of four light Higgsinos $\tilde{W}_1^{\pm}$ and $\tilde{Z}_{1,2}$ similar to RNS models. However, in contrast to RNS models, the third generation squarks tend to be lighter (although not as light as generic natural SUSY which favors $m_{\tilde{t}_{1,2}} \lesssim 500$ GeV). The lighter third generation squarks lead to significant SUSY contributions to the decay $b \to s\gamma$ and seem to be disfavored by the measured value of this branching fraction. In the case of low $\Delta_{\rm HS}$ models, the lightest neutralino is more Higgsino-like than in RNS models, leading to even lower values of predicted relic density and low direct detection rates. The remaining CDM abundance may be augmented by scalar field or axino/saxion production and decay in the early universe, and in the latter case, the additional presence of axions is expected.

ACKNOWLEDGMENTS

We thank P. Huang, D. Mickelson, A. Mustafayev and X. Tata for previous collaborations leading up to this study. This work was supported in part by the U. S. Department of Energy, Office of High Energy Physics.

[1] L. E. Ibañez and G. G. Ross, Phys. Lett. **110B**, 215 (1982); K. Inoue, A. Kakuto, H. Komatsu, and S. Takeshita, Prog. Theor. Phys. **68**, 927 (1982); **71**, 413 (1984); L. Ibañez, Phys. Lett. **118B**, 73 (1982); J. Ellis, J. Hagelin, D. Nanopoulos, and M. Tamvakis, Phys. Lett. **125B**, 275 (1983); L. Alvarez-Gaumé, J. Polchinski, and M. Wise, Nucl. Phys. **B221**, 495 (1983).

[2] G. Aad *et al.* (ATLAS Collaboration), Phys. Lett. B **716**, 1 (2012).

[3] S. Chatrchyan *et al.* (CMS Collaboration), Phys. Lett. B **716**, 30 (2012).

[4] H. Baer and X. Tata, *Weak Scale Supersymmetry: From Superfields to Scattering Events* (Cambridge University Press, Cambridge, England, 2006).

[5] M. S. Carena and H. E. Haber, Prog. Part. Nucl. Phys. **50**, 63 (2003).

[6] S. P. Martin, in *Perspectives on Supersymmetry II*, edited by G. L. Kane (World Scientific, Singapore, 2010), pp. 1–153.

[7] A. Chamseddine, R. Arnowitt, and P. Nath, Phys. Rev. Lett. **49**, 970 (1982); R. Barbieri, S. Ferrara, and C. Savoy, Phys. Lett. **119B**, 343 (1982); N. Ohta, Prog. Theor. Phys. **70**, 542 (1983); L. Hall, J. Lykken, and S. Weinberg, Phys. Rev. D **27**, 2359 (1983); V. D. Barger, M. S. Berger, and P. Ohmann, Phys. Rev. D **47**, 1093 (1993); G. Kane, C. Kolda, L. Roszkowski, and J. Wells, Phys. Rev. D **49**, 6173 (1994).

[8] R. Barbieri and A. Strumia, Phys. Lett. B **433**, 63 (1998).

[9] See, e.g., M. Shifman, Mod. Phys. Lett. A **27**, 1230043 (2012).

[10] J. R. Ellis, K. Enqvist, D. V. Nanopoulos, and F. Zwirner, Mod. Phys. Lett. A **1**, 57 (1986).

[11] R. Barbieri and G. Giudice, Nucl. Phys. **B306**, 63 (1988).

[12] G. L. Kane, C. F. Kolda, L. Roszkowski, and J. D. Wells, Phys. Rev. D **49**, 6173 (1994).

[13] G. W. Anderson and D. J. Castano, Phys. Lett. B **347**, 300 (1995); Phys. Rev. D **52**, 1693 (1995).

[14] S. Dimopoulos and G. Giudice, Phys. Lett. B **357**, 573 (1995).

[15] P. H. Chankowski, J. R. Ellis, and S. Pokorski, Phys. Lett. B **423**, 327 (1998); P. H. Chankowski, J. R. Ellis, M. Olechowski, and S. Pokorski, Nucl. Phys. **B544**, 39 (1999).

[16] K. L. Chan, U. Chattopadhyay, and P. Nath, Phys. Rev. D **58**, 096004 (1998).

[17] G. L. Kane and S. F. King, Phys. Lett. B **451**, 113 (1999); M. Bastero-Gil, G. L. Kane, and S. F. King, Phys. Lett. B **474**, 103 (2000).

[18] J. L. Feng, K. T. Matchev, and T. Moroi, Phys. Rev. D **61**, 075005 (2000); J. L. Feng and K. T. Matchev, Phys. Rev. D **63**, 095003 (2001); J. L. Feng, K. T. Matchev, and D. Sanford, Phys. Rev. D **85**, 075007 (2012); J. L. Feng and D. Sanford, Phys. Rev. D **86**, 055015 (2012).

[19] O. Lebedev, H. P. Nilles, and M. Ratz, arXiv:hep-ph/0511320.

[20] H. Abe, T. Kobayashi, and Y. Omura, Phys. Rev. D **76**, 015002 (2007).

[21] S. P. Martin, Phys. Rev. D **75**, 115005 (2007).

[22] S. Antusch, L. Calibbi, V. Maurer, M. Monaco, and M. Spinrath, J. High Energy Phys. 01 (2013) 187.

[23] M. Perelstein and B. Shakya, J. High Energy Phys. 10 (2011) 142; arXiv:1208.0833.

[24] For a recent review, see e.g. J. L. Feng, arXiv:1302.6587.

[25] H. Baer, V. Barger, P. Huang, A. Mustafayev, and X. Tata, Phys. Rev. Lett. **109**, 161802 (2012); H. Baer, V. Barger, P. Huang, D. Mickelson, A. Mustafayev, and X. Tata, Phys. Rev. D **87**, 115028 (2013).

[26] J. Ellis, K. Olive, and Y. Santoso, Phys. Lett. B **539**, 107 (2002); J. Ellis, T. Falk, K. Olive, and Y. Santoso, Nucl. Phys. **B652**, 259 (2003); H. Baer, A. Mustafayev, S. Profumo, A. Belyaev, and X. Tata, J. High Energy Phys. 07 (2005) 065.

[27] R. Kitano and Y. Nomura, Phys. Lett. B **631**, 58 (2005); Phys. Rev. D **73**, 095004 (2006).

[28] M. Papucci, J. T. Ruderman, and A. Weiler, J. High Energy Phys. 09 (2012) 035.

[29] C. Brust, A. Katz, S. Lawrence, and R. Sundrum, J. High Energy Phys. 03 (2012) 103; R. Essig, E. Izaguirre, J. Kaplan, and J. G. Wacker, J. High Energy Phys. 01 (2012) 074.

[30] H. Baer, V. Barger, P. Huang, D. Mickelson, A. Mustafayev, and X. Tata, Phys. Rev. D **87**, 035017 (2013).

[31] H. Baer, A. D. Box, and H. Summy, J. High Energy Phys. 10 (2010) 023.

[32] A. Djouadi, J.-L. Kneur, and G. Moultaka, Comput. Phys. Commun. **176**, 426 (2007); J. Conley, S. Gainer, J. Hewett, M. Le, and T. Rizzo, Eur. Phys. J. C **71**, 1697 (2011); S. Sekmen, S. Kraml, J. Lykken, F. Moortgat, S. Padhi, L. Pape, M. Pierini, H. B. Prosper, and M. Spiropulu, J. High Energy Phys. 02 (2012) 075; M. W. Cahill-Rowley, J. L. Hewett, A. Ismail, and T. G. Rizzo, Phys. Rev. D **88**, 035002 (2013); C. Boehm, P. S. B. Dev, A. Mazumdar, and E. Pukartas, J. High Energy Phys. 06 (2013) 113.

[33] I. Gogoladze, F. Nasir, and Q. Shafi, Int. J. Mod. Phys. A **28**, 1350046 (2013).

[34] ISAJET, by H. Baer, F. Paige, S. Protopopescu, and X. Tata, arXiv:hep-ph/0312045.

[35] H. Baer, C. H. Chen, R. Munroe, F. Paige, and X. Tata, Phys. Rev. D **51**, 1046 (1995); H. Baer, J. Ferrandis, S. Kraml, and W. Porod, Phys. Rev. D **73**, 015010 (2006).

[36] J. Hisano, H. Murayama, and T. Yanagida, Nucl. Phys. **B402**, 46 (1993); Y. Yamada, Z. Phys. C **60**, 83 (1993); J. L. Chkareuli and I. G. Gogoladze, Phys. Rev. D **58**, 055011 (1998).

[37] S. Martin and M. Vaughn, Phys. Rev. D **50**, 2282 (1994).

[38] Y. Yamada, Phys. Lett. B **316**, 109 (1993); Phys. Rev. Lett. **72**, 25 (1994); Phys. Rev. D **50**, 3537 (1994).

[39] H. Haber and R. Hempfling, Phys. Rev. D **48**, 4280 (1993).

[40] D. Pierce, J. Bagger, K. Matchev, and R. Zhang, Nucl. Phys. **B491**, 3 (1997).

[41] F. Gabbiani, E. Gabrielli, A. Masiero, and L. Silvestrini, Nucl. Phys. **B477**, 321 (1996).

[42] Joint LEP 2 Supersymmetry Working Group, Combined LEP Chargino Results up to 208 GeV, http://lepsusy.web.cern.ch/lepsusy/www/inos_moriond01/charginos_pub.html.

[43] V. Barger, M. Berger, and R. J. N. Phillips, Phys. Rev. Lett. **70**, 1368 (1993); J. Hewett, Phys. Rev. Lett. **70**, 1045 (1993).

[44] H. Baer and M. Brhlik, Phys. Rev. D **55**, 3201 (1997); H. Baer, M. Brhlik, D. Castano, and X. Tata, Phys. Rev. D **58**, 015007 (1998).

[45] S. R. Choudhury and N. Gaur, Phys. Lett. B **451**, 86 (1999); K. S. Babu and C. F. Kolda, Phys. Rev. D **84**, 228 (2000); our calculation uses the formulas in J. Mizukoshi, X. Tata, and Y. Wang, Phys. Rev. D **66**, 115003 (2002).

[46] D. Asner *et al.* (Heavy Flavor Averaging Group), arXiv:1010.1589.

[47] M. Misiak *et al.*, Phys. Rev. Lett. **98**, 022002 (2007).

[48] R. Aaij *et al.* (LHCb Collaboration), Phys. Rev. Lett. **110**, 021801 (2013).

[49] H. Baer, V. Barger, and P. Huang, J. High Energy Phys. 11 (2011) 031.

[50] D. Eriksson, F. Mahmoudi, and O. Stal, J. High Energy Phys. 11 (2008) 035.

[51] Y. Amhis *et al.* (Heavy Flavor Averaging Group Collaboration), arXiv:1207.1158.

[52] J. P. Lees *et al.* (*BABAR* Collaboration), Phys. Rev. Lett. **109**, 101802 (2012).

[53] K. Nakamura (Particle Data Group Collaboration), J. Phys. G **37**, 075021 (2010).

[54] A. Freitas and Y.-C. Huang, J. High Energy Phys. 08 (2012) 050; 05 (2013) 074.
[55] M. Boulware and D. Finnell, Phys. Rev. D **44**, 2054 (1991).
[56] J. D. Wells, C. F. Kolda, and G. L. Kane, Phys. Lett. B **338**, 219 (1994).
[57] J. D. Wells and G. L. Kane, Phys. Rev. Lett. **76**, 869 (1996).
[58] IsaReD, see H. Baer, C. Balazs, and A. Belyaev, J. High Energy Phys. 03 (2002) 042.
[59] P. A. R. Ade *et al.* (Planck Collaboration), arXiv:1303.5076.
[60] T. Moroi and L. Randall, Nucl. Phys. **B570**, 455 (2000); G. Gelmini and P. Gondolo, Phys. Rev. D **74**, 023510 (2006); G. Gelmini, P. Gondolo, A. Soldatenko, and C. Yaguna, Phys. Rev. D **74**, 083514 (2006); **76**, 015010 (2007); B. Acharya, K. Bobkov, G. Kane, P. Kumar, and J. Shao, Phys. Rev. D **76**, 126010 (2007); **78**, 065038 (2008); B. Acharya, P. Kumar, K. Bobkov, G. Kane, J. Shao, and S. Watson, J. High Energy Phys. 06 (2008) 064; R. Allahverdi, B. Dutta, and K. Sinha, Phys. Rev. D **86**, 095016 (2012).
[61] K. J. Bae, H. Baer, and A. Lessa, J. Cosmol. Astropart. Phys. 04 (2013) 041.
[62] H. Baer, C. Balazs, A. Belyaev, and J. O'Farrill, J. Cosmol. Astropart. Phys. 09 (2003) 007.
[63] E. Aprile *et al.* (XENON100 Collaboration), Phys. Rev. Lett. **109**, 181301 (2012).
[64] H. Baer, V. Barger, and D. Mickelson, arXiv:1303.3816.